Catalysis Today 164 (2011) 370–376

Contents lists available at ScienceDirect

Catalysis Today

journal homepage: www.elsevier.com/locate/cattod

Preparation and characterisation of mesoporous photoactive Na-titanate microspheres

Ibrahim El Saliby [a], Laszlo Erdei [b], Ho Kyong Shon [a,*], Jong Beom Kim [c], Jong-Ho Kim [c]

[a] Faculty of Engineering and Information Technology, University of Technology Sydney, NSW 2007, Australia
[b] Faculty of Engineering and Surveying, University of Southern Queensland, QLD 4350, Toowoomba, Australia
[c] The Research Institute for Catalysis, Chonnam National University, Gwangju 500-757, South Korea

ARTICLE INFO

Article history:
Received 1 July 2010
Received in revised form 6 November 2010
Accepted 9 November 2010
Available online 8 December 2010

Keywords:
Na-titanate
Methylene blue
Microspheres
Mesoporous
Titanium dioxide

ABSTRACT

Mesoporous Na-titanate microspheres were fabricated by a simple low temperature hydrothermal synthesis. Microspheres were obtained after treating TiO_2 (Degussa P-25) with a mixture of sodium hydroxide (NaOH) and hydrogen peroxide (H_2O_2) at 25 °C and 80 °C. The as-prepared powders were characterised by X-ray diffraction, N_2 adsorption–desorption measurements and scanning electron microscope/energy dispersive X-ray spectroscopy. The as-prepared microspheres were calcined at 550 °C to investigate the effect of calcination on morphology and characteristics. Microspheres were tested for the adsorption and photodecomposition of methylene blue (MB) under ultraviolet light. The results revealed that microspheres with average diameter of 700 nm were formed by self-assembly of tiny TiO_2 nanoparticles during the reaction at 25 °C, whereas spherical aggregation of nanofibres was detected in powders produced at 80 °C. Calcination of samples had low impact on morphology, adsorption and photocatalytic degradation of MB. These novel materials are effective adsorbents of MB, and also capable of its photodecolorisation.

1. Introduction

Photocatalysis over semiconductors has been widely studied in the past few decades. Generally, titania (TiO_2) is well known as a leader photocatalyst and has been extensively studied under different conditions and for many applications. The ultra-violet light irradiation of titanate nanomaterials is sufficient to initiate the decomposition of organic compounds in aqueous solution, degrade recalcitrant organic pollutants and bleach dye contaminated water [1].

Recent advances in the field of semiconductors show that the synthesis of one-dimensional titanate nanostructures such as nanowires, nanospheres and nanofibres attracts much attention due to their potential use in different applications, mainly photocatalysis. Titanate nanospheres can be obtained by several processes [2–6]. Template synthesis of hollow titania nanospheres was successfully achieved by using a cationic colloidal template as reported by Kim et al. [2]. Negatively charged titania precursors were hydrolysed onto the cationic colloidal particles, which were subsequently removed by heating at 450 °C to obtain hollow titania nanospheres. Zhu et al. [3] reported that the fabrication of TiO_2 nanospheres is possible through diffuse coplanar surface discharge-induced plasma chemical vapour deposition process at room temperature and under atmospheric pressure. Crystalline, uniform-sized and photoactive TiO_2 nanosphere films reduced the concentration of formaldehyde from 2.90 mg/L to 2.43 mg/L after 2 h of UV light irradiation [3]. The reactive microemulsion synthesis is considered another powerful method for obtaining nanospheres with controlled shape and size. Shape and size control is achieved by using microemulsions (water, oil and surfactant), which are considered as chemical microreactors [4]. Similarly, spray-hydrolytic synthesis [5] and laser ablation [6] have been employed to synthesise titanate nanospheres. The fabrication of large titania microspheres can also be achieved by spray coating process [7,8], template [9] and H_2O_2-assisted hydrothermal route [10,11]. Hydrogen peroxide is an environmentally friendly solvent and oxidant. It has been widely employed to synthesise inorganic materials under hydrothermal conditions [12]. The adoption of environmentally friendly processes to produce one-dimensional nanostructures is essential for both the sustainability of the production and the protection of the environment. Jiang et al. [10] synthesised hollow anatase TiO_2 microspheres by dissolving commercial titanium powder into a mixture of H_2O_2, water and hydrofluoric acid. The pH of the mixture was adjusted using ammonia before being exposed to a hydrothermal treatment at 180 °C for 24 h. The microspheres had an average diameter of 750 nm, a wall thickness of 80–140 nm, a hollow interior and composed of nanoparticles with diameters of 20–40 nm. On the other hand,

* Corresponding author. Tel.: +61 2 9514 2629; fax: +61 2 9514 2633.
E-mail addresses: ibelsali@eng.uts.edu.au (I. El Saliby), Laszlo.Erdei@usq.edu.au (L. Erdei), hkshon@eng.uts.edu.au (H.K. Shon), mask-k@hanmail.net (J.B. Kim), jonghkim@jnu.ac.kr (J.-H. Kim).

0920-5861/$ – see front matter © 2010 Elsevier B.V. All rights reserved.
doi:10.1016/j.cattod.2010.11.026

hollow rutile microspheres were obtained when using $TiCl_3$ as a titanium source indicating the important role that titanium precursor plays in the morphology and characteristics of the end product [10]. Yada et al. [11] synthesised layered sodium titanate nanofibres and microspheres from a peroxotitanic acid (PTA) solution. PTA was mixed with NaOH and treated hydrothermally at 100–120 °C for 5–72 h. The Na-titanates obtained from PTA partially included peroxo group in the titanium oxyhydroxide framework, have larger amount of Na^+ ions and have more ion exchange sites. The authors also reported that anatase type nanofibres and microspheres were obtained by the protonation of the nanostructured sodium titanate and the subsequent calcination [11].

Nanostructured titanates are gaining popularity in the photocatalytic processes for water treatment because of their remarkable photocatalytic activity and their ease of separation from the solution [7]. Dye pollutants from various industrial processes are considered as a dramatic source of eutrophication, water coloration and ecosystem perturbation [13–15]. Photocatalysis is considered as the only application among several heterogeneous photocatalysis processes, which is capable of decomposing organic pollutants into harmless compounds (CO_2 and H_2O) without heating nor using high pressure oxygen nor requiring chemical reactants and additives [13]. Methylene blue (MB) is a cationic dye and a frequently used model pollutant in bench-scale studies of photocatalysts. Therefore, the pathways of reactions, and the effect of operational parameters (process pH, MB and catalyst concentration, and photonic flux) on reaction kinetics are well established [1,13,16–18].

In the present article, it was attempted to synthesise titanate microspheres by a simple approach, which employs environmentally friendly compounds and relatively low temperature hydrothermal conditions. A modified peroxotitanate synthesis employing sodium hydroxide as a strong base for nanostructure fabrication was adopted in this process. Microspheres were characterised and tested for the adsorption and photocatalytic activity using MB as a model water pollutant.

2. Experimental

2.1. Materials

Degussa P-25 commercial titanium dioxide was used as a precursor for the preparation of Na-titanate microspheres. P-25 is a non-porous, mixed phase catalyst with 70% anatase and 30% rutile composition and with a BET surface area of 50 m^2/g that corresponds to a mean particle size of about 30 nm. Hydrogen peroxide (50%, w/w) was obtained from Australian Scientific Pty Ltd., hydrochloric acid (37%, v/v) from Scharlau chemie S.A., ethanol (analytical reagent, 96%) from UNIVAR Australia Pty Ltd., sodium hydroxide (97%, w/w) and methylene blue (96%, w/w) from Chem-Supply Pty Ltd. Ultrapure (Milli Q) water was used for making up solutions and washing prepared powder samples.

2.2. Synthesis

In a typical synthesis of Na-titanates, a modified peroxotitanate method was adopted, which involved the mixing of 2 g of P-25 powder with 12 mL of H_2O_2 and 4 g of NaOH so the final pH of the mixture was around 13 [11,19,20]. The mixture was homogenised using a magnetic stirrer and placed in a Teflon-coated Pyrex container at two different temperatures (25 and 80 °C) for 24 h. After the hydrothermal treatment, the solids were recovered by centrifugation (Centurion Sci., 2040) at 3000 rpm for 5 min, washed with 1N HCl solution and Milli Q water until pH 7, and then dried in oven at 75 °C for 24 h. The obtained products are denoted hereafter NT-xx, where xx indicates the temperature of the synthesis. Some samples were also calcined in a furnace (Labec, CE-MLS) at 550 °C for 4 h, thus are designated by NTC-xx.

2.3. Nanomaterial characterisation

Morphology and elemental composition analyses were carried out using a scanning electron microscope equipped with an energy dispersive X-ray detector (Zeiss Supra 55VP SEM) operating at 20 kV. X-ray diffraction (XRD) patterns were generated on a MDI Jade 5.0 (MaterialsData Inc., USA) X-ray diffractometer with Cu Kα radiation source. The data were measured within the range of scattering angle 2θ of 5–90°. The powders of the specimens were used without further treatment. Brunauer, Emmet and Teller (BET) surface area analyses were performed on an automated surface area analyser (Micromeritics Gemini 2360, USA) by means of nitrogen adsorption–desorption. The BET surface area was determined by a multipoint BET method using the adsorption data in the relative pressure (P/P_0) range of 0.05–0.18. The mean pore diameter and the total pore volume of samples was determined from the desorption isotherm via Barret–Joyner–Halender (BJH) model.

2.4. Adsorptive and photocatalytic properties

MB powder was dissolved in pure water to prepare a stock solution of 10 mg/L concentration and the pH of the solution was adjusted to 7 using 0.1N NaOH. Dye adsorption experiments were carried out in an orbital shaking incubator (TU-400, Thermoline Sci.) operating at 150 rpm and 25 °C for 30 min to reach adsorption equilibrium. Samples were collected and filtered through 0.45 μm (Whatman, regenerated cellulose) syringe filters before analyses.

The photocatalytic activity of the mesoporous microspheres was assessed by batch experiments using a 2-L volume of stock MB solution. After the addition of 0.05 g/L photocatalyst, the slurry was mixed with a magnetic stirrer at 450 rpm for 30 min (dark adsorption). The cylindrical reactor (40 cm × 10 cm) vessel had three (15 W each) immersed UVC lamps (Perkin Elmer), a temperature controlling device and an air sparger (0.6 L/min) to provide dissolved oxygen. Photocatalysis was carried out for 90 min at a stable temperature of 26 °C. Slurry samples were collected at 15 min intervals and analysed for MB decomposition at λ = 664 nm using a Shimadzu UV-Vis1700 spectrophotometer. Dissolved organic carbon (DOC) concentrations were monitored using Multi N/C 3100 (Analytik Jena) DOC analyser. Mineralisation of MB was assessed by sulphate determination in collected samples using a Metrohm ion chromatograph (790 IC) equipped with a Metrosep A Supp 5-150 (150 mm × 4.0 mm, 5 μm) column. The eluent used to run the samples consisted of 1 mmol/L of sodium hydrogen carbonate and 3.2 mmol/L of sodium carbonate dissolved in MQ water. The injection volume was 5 mL and the run time was 22 min.

2.5. Lifetime cycle of photocatalysts

The photocatalytic stability of photocatalysts was studied by running the photodegradation experiments for 5 times under the same experimental conditions described in section 2.4. The circled degradation was monitored by collecting samples at $t = 0$ (after 30 min adsorption), 30, 60 and 90 min of photoreaction and analysed for the decrease of absorbance at λ = 664 nm. After each degradation cycle, the supernatant was poured out from the reactor vessel and the photocatalyst was recovered by centrifugation at 3000 rpm for 5 min. The recovered powder was washed with 0.1N HCl, pure ethanol and MQ water to remove any residual by-products resulting from the photodegradation of MB. After each wash, the powder was separated by centrifugation and finally dried at 80 °C for the next degradation cycle.

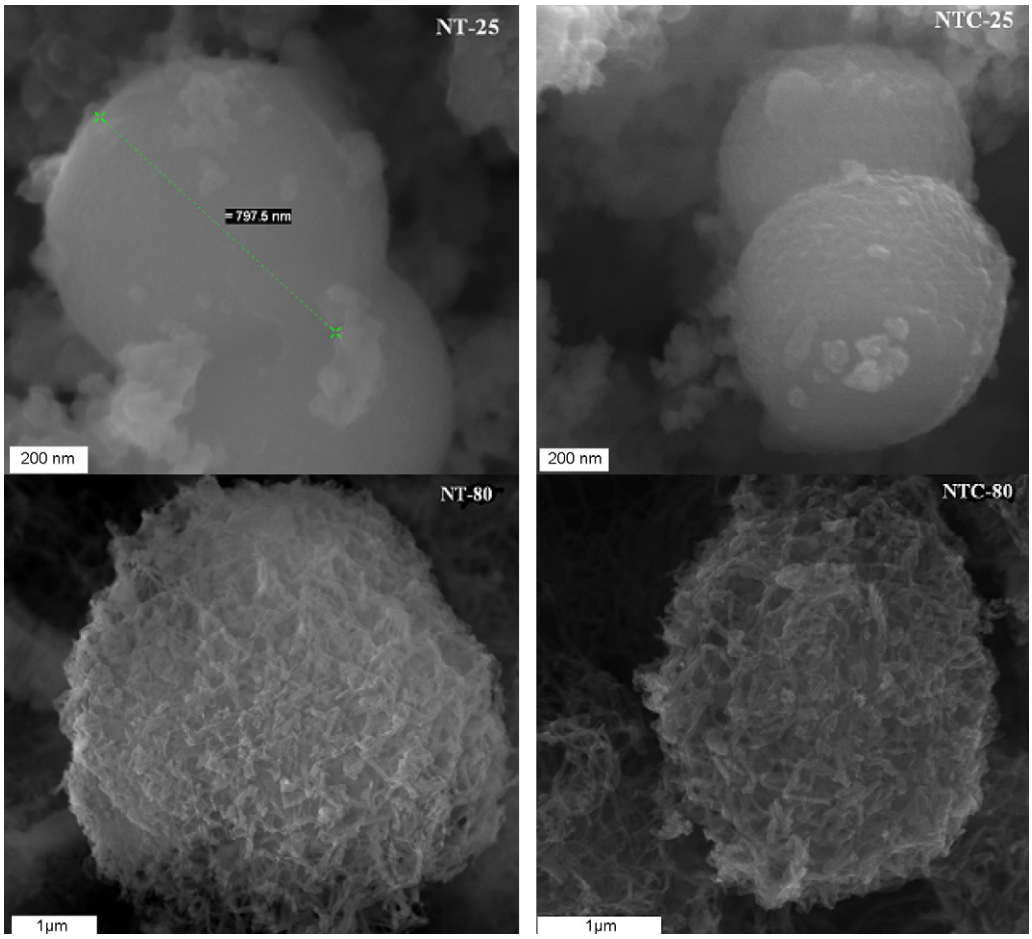

Fig. 1. SEM images of as prepared samples (NT-25 and NT-80) and calcined samples (NTC-25 and NTC-80).

2.6. Separation by settling

The separation of catalysts was studied by monitoring the turbidity of the supernatant as a function of time. The experiment was carried out at 22 °C and neutral pH (6.8–7.2) in the cylindrical reactor described in Section 2.4. A total of 100 mg of catalyst were mixed with 2 L of MQ water; the suspension was stirrer for 5 min then left at static conditions for 2 h to monitor particle settling. Samples were collected at specific time interval (0, 15, 30, 60 and 120 min) at a depth of 10 cm and checked for changes in turbidity. The turbidity was measured using a turbidity and chlorine meter (HI 93414, Hanna instruments, USA), which was calibrated using standard turbidity solutions.

3. Results and discussion

3.1. Characteristics of mesoporous microspheres

The as-prepared titanate powders had pale yellow colour for NT-80 and yellow for NT-25, whereas calcined samples had a white colour and their SEM pictures are shown in Fig. 1. The yellowish colour in NT-25 and NT-80 is due to titanium oxyhydroxide containing peroxo group. After calcination, the peroxo group was lost under the effect of temperature resulting in a white coloured powder [11].

Microspheres of an average 2.5 μm diameter were observed in NT-80 samples, whereas fused/interconnected and independent microspheres (700 nm average in diameter) were found in NT-25 samples. The smooth external surface of NT-25 microspheres suggests that they were formed by the self-assembly and aggregation of countless number of small nanoparticles [21]. On the other hand, fibrous microspheres were produced after the treatment at 80 °C (NT-80, Fig. 1). High magnification micrographs of the surface of microspheres indicated that fibres of few hundred nanometres in length and a diameter in the range of 40–70 nm are present. After calcination, microspheres maintained their shape but the calcination resulted in shrinkages and the average diameter was reduced to 500 nm for smooth surface microspheres and to 1.9 μm for fibrous ones. This decrease in average size of microspheres is due to the collapse of smaller pores and the evaporation of physically adsorbed water particles [5]. Moreover, the smooth surface of microspheres became rough in calcined samples indicating that the crystalline size is significantly increased.

The N_2 adsorption–desorption measurements were employed to investigate the BET surface area, pore structure and pore volume of microspheres. The isotherms of both samples are of type III with two distinct regions (data not shown). The isotherms exhibit a hysteresis loop of type H3, indicating the presence of mesopores [5,22–23]. The shape of these isotherms indicates as well the presence and dominance of slit-shaped pores [23]. After calcination, the isotherms of microspheres were similar to uncalcined samples. The only difference being that the adsorbed volume of N_2 decreased by 30 cm^3/g due to the collapse of few mesopores. The BET specific surface area, the total pore volume and the mean pore diameter of microspheres are presented in Table 1. The increase in surface area in NT-80 can be attributed to the morphology transfer from nanoparticles to nanostructures [24,25]. The samples showed an expected decrease in BET surface areas and total pore volume but

Table 1
Textural parameters of microspheres synthesised in this study.

Nanocatalyst	S_{BET}[a] ($m^2\,g^{-1}$)	V_p[b] ($cm^3\,g^{-1}$)	D_p[c] (Å)
NT-25	24.38	0.16	75.21
NT-80	64.80	0.25	59.85
NTC-25	20.16	0.12	103.21
NTC-80	24.02	0.21	96.96

[a] BET surface area.
[b] Total pore volume.
[c] Mean pore diameter as estimated from nitrogen desorption isotherms using the Barrett–Joyner–Halenda (BJH) model.

an increase in average pore diameter after calcination. The total pore volume decrease is due to the collapse of small pores during the calcination process [5].

The XRD diffraction peaks of NT-80 and NT-25 for 2θ diffraction angles were recorded between 5° and 90°. Five primary peaks of anatase phase at 25.2°, 38°, 48.2° and 55° were recorded, while small diffraction peaks at 54° and 69° indicated the rutile phase. The precursor (P25) is a mixed phase catalyst showing anatase peaks at 25.2°, 38°, 48.2° and 55° and a prominent rutile peak (1 1 0) at $2\theta = 27.45°$. This peak disappeared in NT-25 and NT-80 suggesting that a major part of rutile crystals was dissolved under the experimental conditions [20]. As expected, anatase phase crystals were obtained after calcining NT-25 and NT-80 at 550 °C for 4 h. EDX measurements revealed that the Na to Ti atomic ratio was equal to 0.38 for NT-25 and 0.22 for NT-80. This difference might be due to the binding of Na^+ ions to the negatively charged peroxo group $(Ti_2O_5)_q(OH)_y^{(y-2q)-}$ present more abundantly on NT-25 than NT-80 [11].

3.2. Adsorption of methylene blue on mesoporous microspheres

The adsorption of MB on the surface of the catalysts was studied (Fig. 2A and B). The colour adsorption capacity and the DOC removal of NT-80 and NTC-80 are larger than those of NT-25 and NTC-25. In general, NT-80 showed the highest capacity for MB adsorption followed by NTC-80 > NT-25 > NTC-25. The dispersed powders were coloured blue after mixing them with MB stock solution, indicating that the removal of MB is due to the adsorption of MB molecules on the mesoporous microspheres. After 30 min, the complete decolourisation was reached for NT-80 and NTC-80, which completely adsorbed MB at 0.5 g/L catalyst loading. NT-80 had higher surface area (64.8 m^2/g), bigger pore volume (0.25 cm^3/g) and lower mean pore diameter (59.85 Å) than NT-25 (24.38 m^2/g, 0.16 cm^3/g, 75.21 Å). Similarly, NTC-80 had higher surface area (24.02 m^2/g), bigger pore volume (0.21 cm^3/g) and lower mean pore diameter (96.96 Å) than NTC-25 (20.16 m^2/g, 0.12 cm^3/g, 103.21 Å). Calcination had little negative effect on the adsorption capacity of the fibrous microspheres at low powder loading (0.05 g/L, 0.1 g/L and 0.2 g/L) but no effect on high loading (0.5 g/L). This can be explained by the decrease in surface area, pore volume and the increase of mean pore diameter. The effect of surface area of the catalysts on MB adsorption revealed that microspheres of nanofibrous-assemblies are more effective adsorbent of MB than microspheres composed of the aggregation of nanoparticles. NT-80 having the biggest surface area showed the highest MB adsorption, while NTC-25 (20.16 m^2/g) showed the lowest overall adsorption.

MB adsorption can also be affected by the cation exchange capacity of Na-titanate nanostructures, which show high affinity towards basic and acid dyes [26]. Lee et al. [26] reported that the adsorption capacity may be decreased by exchanging Na^+ with H^+ using washing in acidic solution. MB as a cationic dye can be exchanged with Na^+ ions, which are incorporated in the crystal matrix of TiO_2 or Na-titanate. EDX results as shown in Section 3.1 revealed that the amount of sodium present in NT-25 is larger than

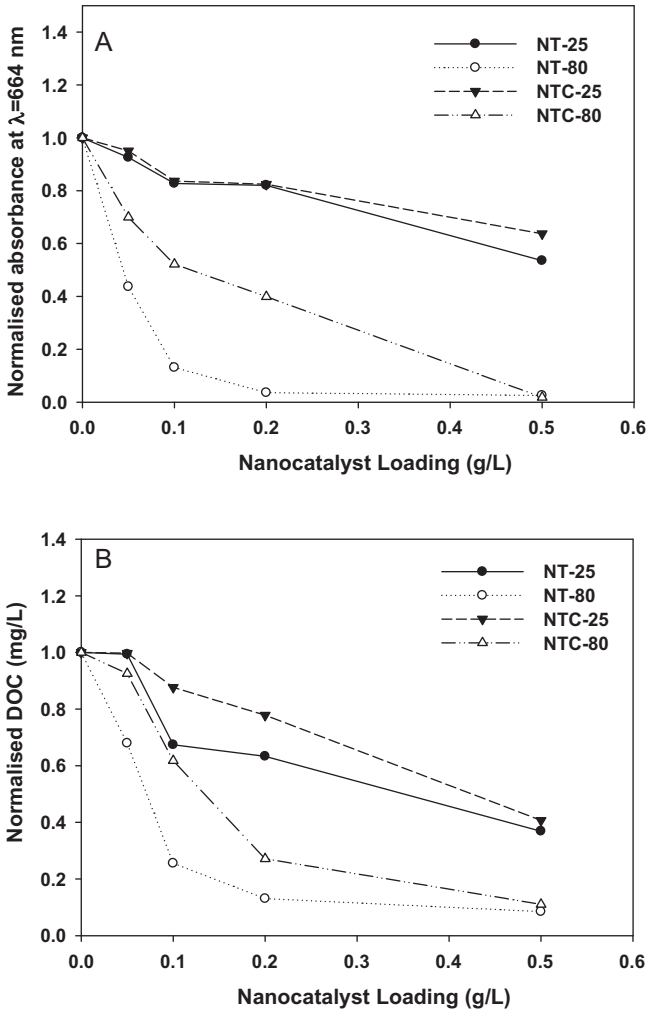

Fig. 2. (A) Decolourisation and (B) DOC removal of MB by adsorption on NT-80, NTC-80, NT-25 and NTC-25 ([MB] = 10 mg/L, pH 7, data collected after 30 min).

that in NT-80. However, the adsorption of these sodium cations on the negatively charged peroxo group reduced its availability for exchange. Here as well, the negatively charged peroxo group $(Ti_2O_5)_q(OH)_y^{(y-2q)-}$ was saturated by the strong binding to Na^+ ions in the titanate framework, which made them also unavailable as a possible boost for adsorption [11,26]. Hence, NT-25 having more less-available peroxo groups and little Na^+ ready for exchange was less efficient in adsorbing MB than NT-80. After the hydrothermal reaction at 80 °C, this binding was lost resulting in the decrease in peroxo groups. This was detected by the change in colour which turned into pale yellow. Consequently, Na^+ was leached away by pure water washings of the powders, which explains the decrease of Na^+ concentration in NT-80.

Photocatalysts load of 50 mg/L were adopted in the rest of the study to minimise the effect of adsorption on photocatalysis results.

3.3. Photocatalytic decolourisation of methylene blue and DOC removal

Fig. 3A and B shows the kinetics of the photocatalytic degradation of MB under UV light. MB was adsorbed onto the catalysts surface for 30 min in dark conditions before the UV lamps were turned on. The decolourisation of NT-80 slurry was complete after 90 min illumination, and was around 85% for NTC-80, NT-25 and NTC-25. This complete decolourisation was due to the high adsorption capacity of NT-80, which adsorbed 50% of MB at equilibrium.

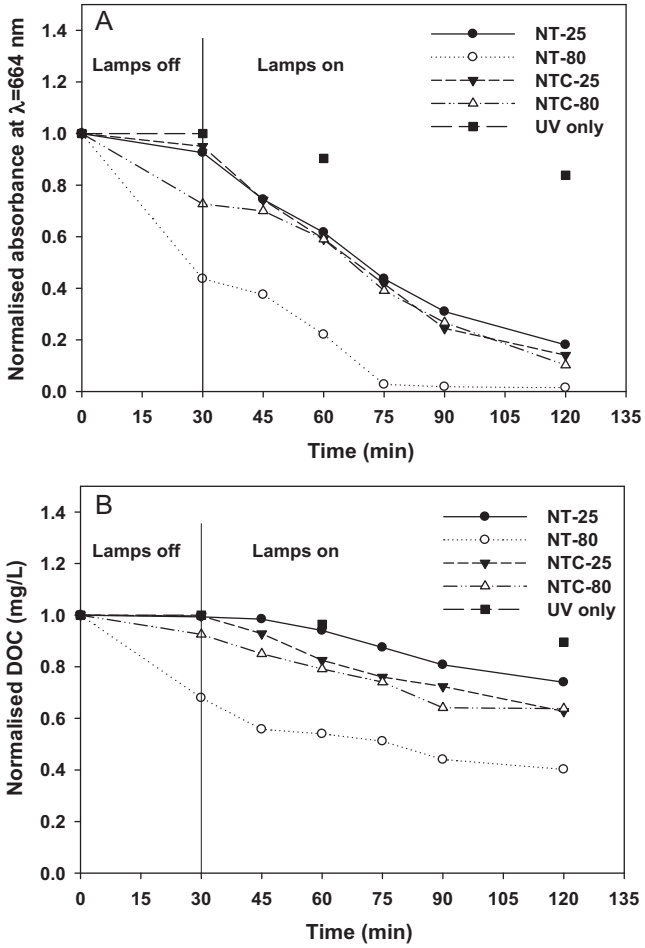

Fig. 3. Kinetics of (A) decolourisation of MB and (B) DOC photodegradation on NT-80, NTC-80, NT-25 and NTC-25 ([MB] = 10 mg/L, pH 7, photocatalyst loading = 50 mg/L).

Low correlations between the decolourisation and the decrease of DOC was detected in all tested samples, suggesting the limited use of the absorbance data to measure organic matter removal. In the present work, baseline experiments showed that UV illumination alone (i.e. in the absence of catalyst) for 90 min reduced the characteristic adsorption peak at 664 nm by 17%. Redox potential measurements and DOC reduction by 11% (Fig. 3A and B) confirmed that the decolourisation was due to chemical degradation rather than temporary colour change.

Heterogenous photocatalysis over TiO_2 follows a well-defined mechanism, which is initiated by the adsorption of efficient photons by titania, and is maintained through a series of reactions that involve the production of positives holes (h^+) and hydroxyl radicals ($OH^\bullet$) [13,27]. The photooxidation of organic compounds is thus reached via successive attacks by $OH^\bullet$. In the present study, MB removal was assessed based on the decrease in the absorbance at 664 nm and the decrease in DOC. The results showed that NT-80 was the best photocatalyst in terms of MB decolourisation and DOC removal. Relative absorbance was reduced by 50% and the DOC was reduced by 30% after 45 min of UV irradiation. The removal of MB using mesoporous microspheres decreased in the order NT-80 > NTC-80 > NT-25 > NTC-25. The calcination of the powders had negative effect on the increase of the photoactivity of the catalysts, which can be ascribed to the changes in morphology. Microspheres had lower BET surface area and pore volume after calcination, which decreased their photocatalytic activity. P25 was used a reference photocatalyst and showed 95% decolourisation of MB solution and 85% DOC removal after 1 h of UV-irradiation at 50 mg/L load.

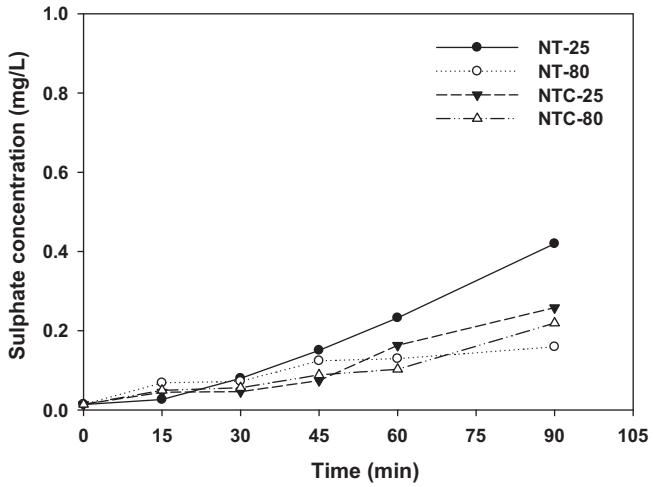

Fig. 4. Evolution of sulphate ions during the photocatalytic degradation of MB over NT-25, NTC-25, NT-80 and NTC-80 ([MB] = 10 mg/L, pH 7, photocatalyst loading = 50 mg/L).

3.4. Mineralisation of methylene blue

The initial step of MB degradation is due to the cleavage of the bonds of the C–S^+=C functional group in MB. This will result in the formation of sulphate ions probably via the formation of a sulfoxide as an intermediate compound as reported by Houas et al. [13]. In the photocatalytic degradation of MB over titania, two oxidative agents can be considered: (i) photo-produced holes h^+ and (ii) the strongly active $OH^\bullet$ radicals. In MB degradation, h^+ are not involved by the initial step (cleavage of the bonds of the C–S^+=C) of degradation as MB is a cationic dye and not an electron donor. So, $OH^\bullet$ radicals are essential for the initiation of the MB dissociation, which will be degraded through a set of chemical reactions described in details by Houas et al. [13]. The end of the mineralisation is attained when the sulphur reaches its final maximum oxidation degree (+6) and SO_4^{2-} is produced after a 4th attack from $OH^\bullet$ radicals on the final by-product: R–C_6H_4–SO_3H [13].

$$R\text{–}C_6H_4\text{–}SO_3H + OH^\bullet \rightarrow R\text{–}C_6H_4 + SO_4^{2-} + 2H^+$$

Thus, the increase in sulphate concentration in the solution indicates the mineralisation of MB. The evolution of sulphate ions was monitored and is presented in Fig. 4.

NT-25 showed the highest mineralisation compared to NTC-25, NT-80 and NTC-80. The suppressed mineralisation of NT-80 and NTC-80 might be due to their high adsorption capacity, which might have saturated the active sites with MB molecules prohibiting the light photons from reaching them. This implies that the degradation process was concurrent with the adsorption process, indicating that the DOC removal and decolourisation of MB was due to sorption and photooxidation at the same time. NT-80 is a strong adsorbent of MB, but showed the lowest mineralisation implying that new MB molecules were adsorbed on the powders after others have been decomposed. On the other hand, NT-25 is a weak adsorbent but had the highest mineralisation, which indicates that a high percentage of decolourisation and DOC removal was due to photooxidation.

3.5. Lifetime cycle of microspheres

The lifecycle of microspheres was monitored over five consecutive photodegradation cycles of MB solution (10 mg/L) at 50 mg/L photocatalyst load (Fig. 5). The photocatalyst was recovered after each cycle by sedimentation, washed, separated by centrifugation and dried at 80 °C before being used in the next cycle. All tested photocatalysts showed stability in performance after 5 runs of MB

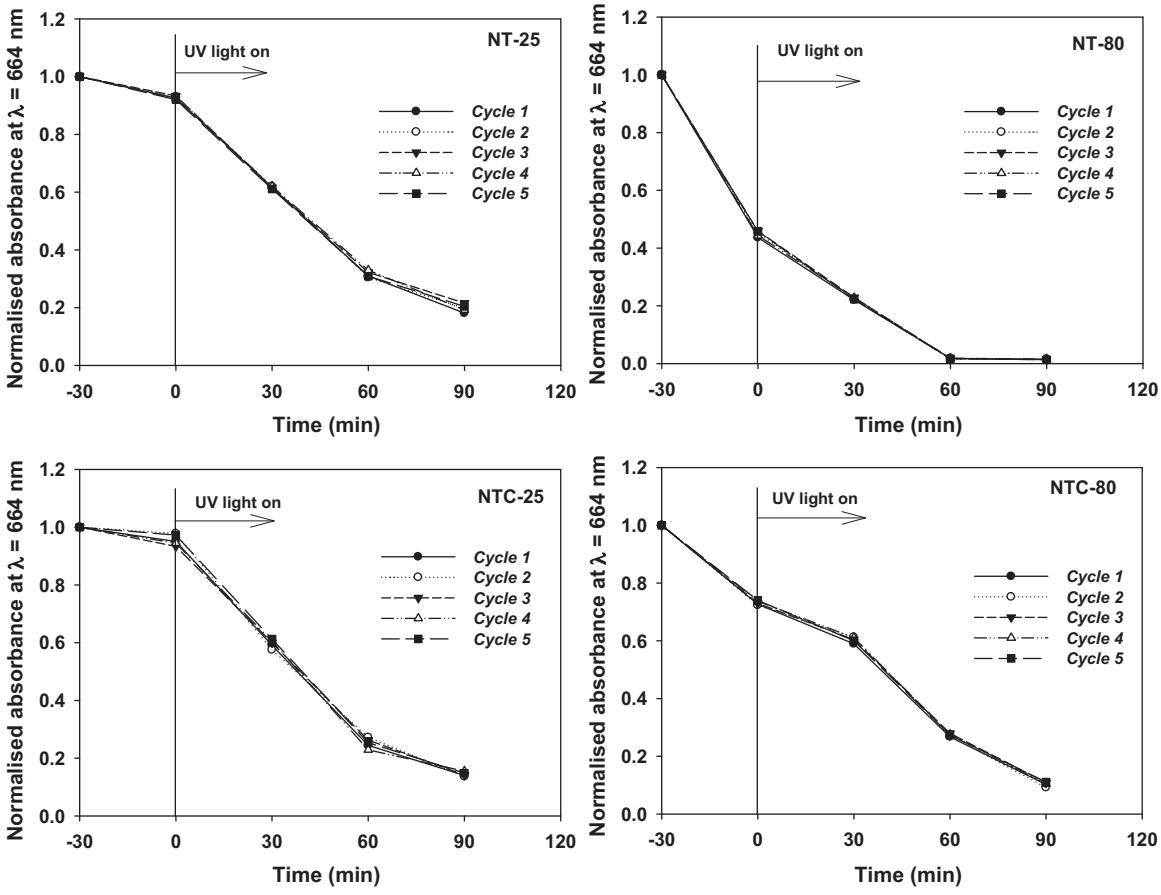

Fig. 5. Lifetime cycles of NT-25, NTC-25, NT-80 and NTC-80 for the decolourisation of MB ([MB] = 10 mg/L, pH 7, photocatalyst loading = 50 mg/L).

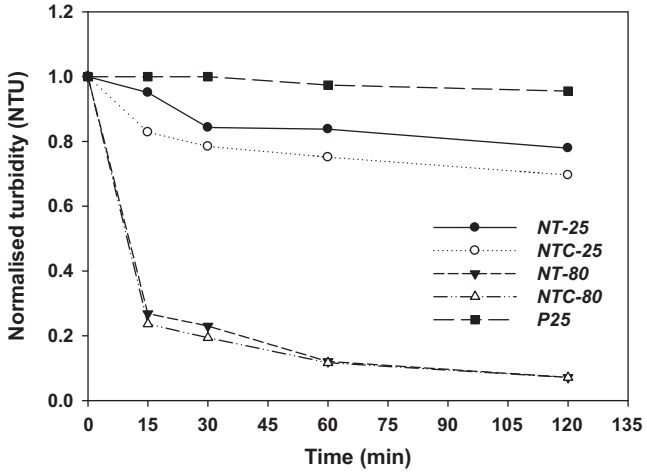

Fig. 6. Normalised decrease in the supernatant turbidity using NT-25, NTC-25, NT-80, NTC-80 and P-25 (pH 7, photocatalyst loading = 50 mg/L).

decomposition. The overall reduction of photocatalytic activity was below 5% according to absorbance results at λ = 664 nm. Thus, the repeated use of microspheres does not poison their photocatalytic activity and elucidate that the powders remain UV light responsive.

3.6. Supernatant turbidity

Post separation of photocatalysts is a real encumber to the success of photocatalytic water treatment processes. In this study, synthesised photocatalysts were tested for their ability to separate from the solution using a cost-effective method, namely sedimentation. Turbidity measurement, which is used to assess the amount of suspended particles in solution, was used to monitor the sedimentation of photocatalysts at 50 mg/L load. The decrease in solution turbidity over time indicates an increase in the sedimentation rate of suspended particles. Normalised turbidity figures were plotted to compare different photocatalysts (Fig. 6). After 2 h at static conditions, the decrease in solution turbidity was around 95% for NT-80 and NTC-80, while it was recorded as 20% and 25% for NT-25 and NTC-25, respectively. On the other hand, the turbidity of the water/P25 suspension remained relatively unchanged with only a 5% decrease in turbidity after 2 h at static conditions. Nanofibrous micorpsheres can be quickly and easily separated from the solution by sedimentation due to their bigger size and fibrous morphology.

4. Conclusion

Na-titanate nanostructures were synthesised using a simple and facile method at low temperatures. Mesoporous smooth surface microspheres with average diameter of 700 nm can be produced by the simple treatment of P25 with NaOH and H_2O_2 at room temperature. Larger size fibrous microspheres result from this treatment at 80 °C. Microspheres showed high affinity in adsorbing MB, which was mainly due to the high surface area of NT-80. The binding of Na^+ and peroxo groups had detrimental effect on the adsorption of the cationic dye because of surface saturation, which decreased the adsorption sites. The decolourisation, DOC removal revealed their photocatalytic activity under UV light irradiation. Moreover, mineralisation of MB was studied for sulphate evolution, which confirmed the positive photocatalytic activity of the microspheres.

Therefore, these novel mesoporous microspheres are considered as effective adsorbents of MB, and also capable of its photocatalytic degradation. Their photocatalytic activity is consistent after 5 photocatalytic runs and they can be easily separated from the solution by settling.

Acknowledgments

This research was funded by ARC-LP, a UTS internal grant and Australian Postgraduate Award scholarship. This work was supported by Priority Research Centers Program through the National Research Foundation of Korea (NRF) funded by the Ministry of Education, Science and Technology (2009-0094057) and the Center for Photonic Materials and Devices at Chonnam National University. This subject is supported by Korea Ministry of Environment as "Converging technology project".

References

[1] H. Lachheb, E. Puzenat, A. Houas, M. Ksibi, E. Elaloui, C. Guillard, J.-M. Herrmann, Photocatalytic degradation of various types of dyes (Alizarin S, Crocein Orange G, Methyl Red, Congo Red, Methylene Blue) in water by UV-irradiated titania, Appl. Catal. B: Environ. 39 (1) (2002) 75–90.
[2] T.H. Kim, K.H. Lee, Y.K. Kwon, Monodisperse hollow titania nanospheres prepared using a cationic colloidal template, J. Colloid Interface Sci. 304 (2006) 370–377.
[3] A.-M. Zhu, L.-H. Nie, Q.-H. Wu, X.-L. Zhang, X.-F. Yang, Y. Xu, C. Shi, Crystalline, uniform-sized TiO_2 nanosphere films by a novel plasma CVD process at atmospheric pressure and room temperature, Chem. Vapor Depos. 13 (2007) 141–144.
[4] F.A. Deorsola, D. Vallauri, Study of the process parameters in the synthesis of TiO_2 nanospheres through reactive microemulsion precipitation, Powder. Technol. 190 (2009) 304–309.
[5] M. Zhou, J. Yu, S. Liu, P. Zhai, B. Huang, Spray-hydrolytic synthesis of highly photoactive mesoporous anatase nanospheres for the photocatalytic degradation of toluene in air, Appl. Catal. B: Environ. 89 (2009) 160–166.
[6] F. Tian, J. Sun, J. Yang, P. Wu, H.-L. Wang, X.-W. Du, Preparation and photocatalytic properties of mixed-phase titania nanospheres by laser ablation, Mater. Lett. 63 (2009) 2384–2386.
[7] P.F. Lee, X. Zhang, D.D. Sun, J. Du, J.O. Leckie, Synthesis of bimodal porous structured TiO_2 microsphere with high photocatalytic activity for water treatment, Colloid Surf. A 324 (2008) 202–207.
[8] X. Zhang, J.H. Pan, A.J. Du, J. Ng, D.D. Sun, J.O. Leckie, Fabrication, Photocatalytic activity of porous TiO_2 nanowire microspheres by surfactant-mediated spray drying process, Mater. Res. Bull. 44 (5) (2009) 1070–1076.
[9] I.A. Kartsonakis, P. Liatsi, I. Danilidis, D. Bouzarelou, G. Kordas, Synthesis, characterization and antibacterial action of hollow titania spheres, J. Phys. Chem. Solids 69 (1) (2008) 214–221.
[10] L. Jiang, Y. Zhong, A simple H_2O_2-assisted route to hollow TiO_2 structures with different crystal structures and morphologies, Mater. Res. Bull. 44 (5) (2009) 999–1002.
[11] M. Yada, Y. Goto, M. Uota, T. Torikai, T. Watari, Layered sodium titanate nanofiber and microsphere synthesized from peroxotitanic acid solution, J. Eur. Ceram. Soc. 26 (4–5) (2006) 673–678.
[12] G. Li, S. Pang, L. Jiang, Z. Guo, Z. Zhang, Environmentally friendly chemical route to vanadium oxide single-crystalline nanobelts as a cathode material for lithium-ion batteries, J. Phys. Chem. B 110 (2006) 9383–9386.
[13] A. Houas, H. Lachheb, M. Ksibi, E. Elaloui, C. Guillard, J.-M. Herrmann, Photocatalytic degradation pathway of methylene blue in water, Appl. Catal. B: Environ. 31 (2) (2001) 145–157.
[14] S. Senthilkumaar, K. Porkodi, R. Gomathi, A.G. Maheswari, N. Manonmani, Sol–gel derived silver doped nanocrystalline titania catalysed photodegradation of methylene blue from aqueous solution, Dyes Pigments 69 (1–2) (2006) 22–30.
[15] M. Vautier, C. Guillard, J.-M. Herrmann, Photocatalytic degradation of dyes in water: case study of indigo and of indigo carmine, J. Catal. 201 (2001) 46–59.
[16] N. Shimizu, C. Ogino, M.F. Dadjour, T. Murata, Sonocatalytic degradation of methylene blue with TiO_2 pellets in water, Ultrason. Sonochem. 14 (2) (2007) 184–190.
[17] C. Ogino, M.F. Dadjour, Y. Iida, N. Shimizu, Decolorization of methylene blue in aqueous suspensions of titanium peroxide, J. Hazard. Mater. 153 (1–2) (2008) 551–556.
[18] I. Moriguchi, M. Honda, T. Ohkubo, Y. Mawatari, Y. Teraoka, Adsorption and photocatalytic decomposition of methylene blue on mesoporous metallosilicates, Catal. Today 90 (3–4) (2004) 297–303.
[19] Y. Mao, M. Kanungo, T. Hemraj-Benny, S.S. Wong, Synthesis and growth mechanism of titanate and titania one-dimensional nanostructures self-assembled into hollow micrometer-scale spherical aggregates, J. Phys. Chem. B 110 (2005) 702–710.
[20] A.Y.L.D. Ohtani, T. Ihara B, R. Abe, Isolation of anatase crystallites from anatase–rutile mixed particles by dissolution with aqueous hydrogen peroxide and ammonia, Trans. Mater. Res. Soc. Jpn. 32 (2007) 401–404.
[21] J. Yu, S. Liu, M. Zhou, Enhanced photocalytic activity of hollow anatase microspheres by Sn^{4+} incorporation, J. Phys. Chem. C 112 (2008) 2050–2057.
[22] International Union of Pure and Applied Chemistry, Recommendations for the characterization of porous solids, Pure Appl. Chem. 66 (8) (1994) 1739–1758.
[23] S. Bordère, P.L. Llewellyn, F. Rouquerol, J. Rouquerol, Multiple features of a porous structure as assessed from the hysteresis of nitrogen adsorption–desorption: case study of the formation of UO_3 from $UO_2(NO_3)_2{\cdot}6H_2O$, Langmuir 14 (15) (1998) 4217–4221.
[24] Wu, et al., Sequence of events for the formation of titanate nanotubes, nanofibers, nanowires and nanobelts, Chem. Mater. 18 (2006) 547–553.
[25] Z.-Y. Yuan, B.-L. Su, Titanium oxide nanotubes, nanofibers and nanowires, Colloid Surf. A 241 (2004) 173–183.
[26] C.-K. Lee, S.-S. Liu, L.-C. Juang, C.-C. Wang, M.-D. Lyu, S.-H. Hung, Application of titanate nanotubes for dyes adsorptive removal from aqueous solution, J. Hazard. Mater. 148 (3) (2007) 756–760.
[27] J.-M. Herrmann, C. Guillard, P. Pichat, Heterogeneous photocatalysis: an emerging technology for water treatment, Catal. Today 17 (1–2) (1993) 7–20.